Comparative Transcriptomic Analysis of the Brain in Takifugu Rubripes Shows Its Tolerance to Acute Hypoxia

Mingxiu Bao
Dalian Ocean University
Fengqin Shang
Dalian Ocean University
Fujun Liu
Dalian Ocean University
Ziwen Hu
Dalian Ocean University
Shengnan Wang
Dalian Ocean University
Xiao Yang
Dalian Ocean University
Yundeng Yu
Dalian Ocean University
Hongbin Zhang
Dalian Ocean University
Chihang Jiang
Dalian Ocean University
Jielan Jiang
Dalian Ocean University
Yang Liu (liuy78@foxmail.com)
Dalian Ocean University https://orcid.org/0000-0002-8195-7706
Xiuli Wang
Dalian Ocean University

Research Article

Keywords: Acute hypoxia, Brain, Transcriptome, Takifugu rubripes, Gene expression

Posted Date: May 25th, 2021

DOI: https://doi.org/10.21203/rs.3.rs-542334/v1

Abstract

Hypoxia is reduced levels of oxygen. Especially in water, due to the complex environment, hypoxic situations often occur. Although fish can survive in low-oxygen waters, this survival ability depends on a complete set of coping mechanisms such as oxygen perception and gene-protein interaction regulation. The research on this mechanism is very meaningful. The present study was undertaken to examine the short-term effects of hypoxia on the brain in *Takifugu rubripes*. We sequenced the transcriptomes of the brain in *T. rubripes* to studied their response mechanism to acute hypoxia. Total 167 genes with adjusted P values<0.05 were differentially expressed in the brain of *T. rubripes* exposed to acute hypoxia. However, *hif1a*, the master transcriptional regulator of the adaptive response to hypoxia, was not significantly regulated, which indicated that the *T. rubripes* brain might prevent the HIF-1 signaling pathway. Then Gene Ontology and KEGG Enrichment Analysis were carried out. The results indicated that hypoxia could cause metabolic and neurological changes, showing the clues of their adaptation to acute hypoxia. Overall, the sequenced transcriptomes of the brain in *T. rubripes* showed small changes under acute hypoxia. As the most complex and important organ, the brain of *T. rubripes* might be able to create a self-protection mechanism to resist or reduce damage caused by acute hypoxia stress.

Introduction

Hypoxia is reduced levels of oxygen. The existence of factors, such as reduced air pressure and poor gas exchange in nature, will cause the occurrence of a hypoxic environment, such as in plateaus(Qiu et al. 2012), aquatic environments(Jackson and Ultsch 2010) , and underground tunnels(Avivi et al. 2005). The animals and plants living in a hypoxic environment have corresponding coping mechanisms in physiology, biochemistry, and behavior. Plants use substances other than oxygen as terminal electron acceptors, and the redox potential in the rhizosphere is reduced. Through a series of physiological and biochemical metabolic reactions, plants can adapt to or alleviate the damage caused by hypoxia stress(Schmidt et al. 2018). Animals have different ways of adapting to different levels of hypoxia: in mild or moderate hypoxic environments, they adjust to the hypoxic environment through the adjustment of the overall horizontal compensation mechanism, such as faster breathing rates, increased pulmonary ventilation, alveolar-blood, and accelerating blood-tissue gas diffusion and strengthening the permanent expansion of capillaries, etc.(Avivi et al. 1999; Liu et al. 2001; Scott 2011; Wan et al. 2013). In severe hypoxic environments, adaptation through overall compensation alone is far from satisfying the body's energy needs, and more importantly, through the adjustment of cell metabolism and the induction of many anti-hypoxic factors adapt to the hypoxic environment at the molecular level. For example, intracellular free calcium increases during hypoxia, then it can activate calcium-related signaling pathways and regulate the increase in transcription of some hypoxia-sensitive genes (Millhorn et al. 1997). *Hif-1* binds to hypoxia-responsive elements (HRE) on its target genes, triggering downstream target genes such as *epo*, inducible nitric oxide synthase (*inos*), *vegf*, and other genes. Transcription affects physiological and pathological processes such as erythropoiesis, angiogenesis, apoptosis, and proliferation, and causes the body to produce a series of adaptive responses to hypoxia (Bruzzi et al.

1997; Erkan et al. 2007). In addition to the hypoxia caused by the reduction of the oxygen content in the environment, many physiological and pathological processes of higher animals also have the phenomenon of hypoxia. For example, in the early stages of mammalian embryonic development, a hypoxic environment is created in the womb. This hypoxic microenvironment is essential for embryo development (Simon and Keith 2008).

Whereas aquatic species (such as fish) are particularly vulnerable to hypoxic conditions, the hypoxic state of aquatic systems usually means that the saturation of dissolved oxygen (DO) is between 0-30% (Pelster and Egg 2018; Wu et al. 2003). The DO concentration in fish ponds depends generally on many factors including photosynthesis of phytoplankton, respiration of aquatic organisms, and/or the diffusion of atmospheric O_2, O_2 partial pressure, water temperature, and salinity. In captivity, fish always face repetitive and chronic stress situations (e.g., confinement, crowding, handling, variable water quality including hypoxia) from which they cannot escape. Across a broad range of fishes, hypoxia can cause direct mortality but more commonly results in various sublethal effects, such as behavioral and physiological stress(Abdel-Tawwab et al. 2019). Hypoxia has been shown to retard growth in bivalves, polychaetes, and fish (Shang and Wu 2004). It also can induce apoptosis(Arend et al. 2011). Fish have developed various adaptation strategies in the long-term evolution process, and their tolerance to hypoxia is very different (Bickler and Buck 2007). Studies have shown that fish could initiate special biological processes and molecular mechanisms in low-oxygen environments, and could more efficiently store and use oxygen through the regulation of key gene expression (Rimoldi et al. 2012). *Salmo salar* could induce vascular endothelial growth factor expression through hypoxia to promote angiogenesis and increase the body's oxygen supply (Vuori et al. 2004). In zebrafish (*Danio rerio*) embryos, gene expression changed in response to hypoxia. *Hif-1a* played an important role in regulating the formation of neural crest and the central nervous system (Ton et al. 2003).

Although there are many studies on molecular mechanisms related to hypoxia, the molecular basis of these adaptations has not been fully understood (Xia et al. 2018). The transcriptome is the sum of all the RNA expressed by a cell or tissue at a specific period. By detecting the expression difference of the transcriptome in different periods and tissues, the gene expression regulation status can be dynamically analyzed (Wilhelm et al. 2008). It is widely used to study the molecular mechanisms of many different species under specific conditions. The transcriptome analysis of *Carassius auratus* showed that the expression of glycolytic pathway-related genes in fish exposed to hypoxia for a long time will be significantly enhanced (Liao et al. 2013). The brain is an oxygen-sensitive organ whose functions are highly susceptible to low oxygen levels (Rahman and Thomas 2015). Also, other studies indicate that the *crucian carp* may be relying on neurotransmitters and neuromodulators to suppress its CNS energy use under hypoxic conditions (Nilsson and Renshaw 2004). Under hypoxic conditions, the expression of hypoxia-inducible factors in the brain tissue of sturgeon increased significantly (Pelster and Egg 2018).

The *T. rubripes* genome sequencing work was completed in 2002. It was found that the *T. rubripes* genome is about 400Mb, which is only one-seventh the size of the human genome. It is the smallest genome of known vertebrates and the number of genes is similar to humans(Brenner et al. 1993; Kai et al.

2011) , so it has been extensively studied as a model organism. We have carried out a simple experiment of acute hypoxia tolerance of *T. rubripes*, which showed that few differentially expressed genes were found (Jiang et al. 2017). In this study, we set four O_2 concentration to detect the transcriptome changes in the brain of *T. rubripes* and aimed to explore the mechanisms of the brain in *T. rubripes* responses to acute hypoxic stress.

Materials And Methods

Experimental animals and acute hypoxia exposure

Animal experiments were approved by the Animal Care and Use committee at Dalian Ocean University. Healthy *T. rubripes* with body weights of 461.75±40.66g were obtained from Dalian Tianzheng Industrial Co., in Dalian, Liaoning, China. Forty fish were randomly selected from the stock and divided equally into four groups kept in 380L tanks with a flow-through seawater supply. The temperature of the water was 19±0.5˚C. Sodium sulfite was used to regulate the DO which was detected by dissolved oxygen meter (Hanna HI9146-04, Romania). The DO of the four tanks (four groups) were maintained at 5.4±0.05 mg O_2/L (ppm5.4), 4±0.05 mg O_2/L (ppm4), 2±0.05 mg O_2/L (ppm2) and 0±0.05mg O_2/L (ppm0). The fish treated by the DO of 5.4±0.05 mg O_2/L (ppm5.4) was considered as control because the DO was same as that in the stock. After 6 hours of treatment, fish were anaesthetized with 80 mg/L concentration of tricaine methane sulfonate (MS-222, Sigma) and then dissected. Brain was obtained and snap-frozen in liquid nitrogen, and then stored at −80°C. Then total RNA was extracted from the brain for the construction of RNA library and qPCR.

Transcript profiling and sequencing (RNAseq)

Total RNA was quantified by the Qubit® RNA Analysis Kit in Qubit® 2.0 (Life Technologies, CA, USA), and its integrity was checked using an Agilent 2100 Bioanalyzer (Agilent Technologies, USA). Twenty RNA (cDNA) libraries (5 biological replicates of each group, including ppm5.4, ppm4, ppm2, and ppm0) were constructed for RNA sequencing and bioinformatics analysis. The library was then sequenced by Novaseq 6000 (Illumina, USA).

Processing of RNAseq data

Raw data were firstly qualified by FastQC (www.bioinformatics.babraham.ac.uk/projects/fastqc/). Clean data (clean reads) were obtained after removing read with containing adapter, ploy-N and low-quality bases by Trimmomatic v0.38 (Bolger et al. 2014). All the downstream analyses were based on clean data. Reference genome (**assembly fTakRub1.2**, www.ncbi.nlm.nih.gov/genome/63) were downloaded from the genome database of NCBI (The National Center for Biotechnology Information). Paired-end clean reads were mapped to the indexed reference genome using Hisat2 v2.1.0 (Kim et al. 2015). The results of mapping were also qualified by FastQC. HTSeq v0.11.2 was used to count the reads mapped to each gene (Anders et al. 2015). Differential gene expression analysis was performed by an R package DESeq2 v3.10 (Love et al. 2014). Principal component analysis (PCA) was performed using an in-house python

script (Supplementary Information File S12). Obtained DEGs were annotated by KOBAS v3.0 (Xie et al. 2011), and subsequently subjected to GO functional enrichment analysis and Kyoto Encyclopedia of Genes and Genomes (KEGG) enrichment analysis by an R package clusterProfiler v3.18.1 (Yu et al. 2012). The software Cytoscape v3.7.1 was used to map the enriched gene and KEGG signaling pathway network interactions (Shannon et al. 2003). Several R packages (ggplot2, pheatmap, venn) were used to draw graphics for the visualization of analyzed data (cran.r-project.org/).

Validation of DEGs by q RT-PCR

Total RNA was extracted from the brain samples using RNAprep pure tissue kit (Tiangen, China). First-strand cDNA was synthesized from 1μg of total RNA using a PrimeScript™ RT Master Mix (Takara, Japan). qPCR was performed using TransStart® Top Green qPCR SuperMix (Transgen, China) on an ABI StepOnePlus™ Real-Time PCR System (Life Technologies, USA). The primers for each gene are listed in Supplementary Information Table S7. The gene expression levels were evaluated relative to the expression level of β-actin using the $2^{-\Delta\Delta CT}$ method (Livak and Schmittgen 2001). The correlation between normalized counts from RNAseq and the relative expression from qPCR was calculated.

Results

Construction of RNA libraries, quality control of raw data

Total 20 libraries were constructed and sequenced from 20 samples in four treatment groups. The average size of insert fragments in these libraries was 275-315 bp (Supplementary Information Table S1). After quality control, clean data from 20 libraries was retained for next step (Supplementary Information Table S2). Total 102.75 Gb clean nucleotides and 685.06 million clean reads were obtained finally. Quality control showed that more than 95% and 89% reads of each sample had the quality scores of Q20 and Q30 (nucleotides with a quality value larger than 20 and 30), respectively. These results indicated our sequencing data were reliable and could be used for further analysis. All clean data was submitted to SRA databases in NCBI (BioProject: PRJNA645780).

Mapping and counting reads

Obtained reads with high quality were mapped to reference genome (Supplementary Information Table S3). Total and unique mapping rates of all samples were more than 92% and 89% respectively. Reads mapped to positive chains of genome were almost equal to that mapped to negative chains. According to the structure of the reference genome, mapped reads were mainly positioned in exons (77-81.5%) (Supplementary Information Table S4). Analysis of mapping results by FastQC showed that the level of duplication in mapped reads was about 15-21% from all samples (Supplementary Information Table S5). These results showed a good mapping quality for further analysis. Then mapped reads in exons were counted by HTSeq (Supplementary Information Table S6).

Analysis of differentially expressed genes (DEGs)

The counted reads by HTSeq were loaded by DESeq2 for differential expression analysis. The results showed that 167 genes were differentially expressed among the different treated groups with adjusted P value <0.05 (Supplementary Information Table S8). But only 19 DEGs with adjusted P value <0.05 and |log2FoldChange|>=1 were obtained (Fig. 1). The comparison group with the highest number of DEGs was ppm0Vsppm5.4, and the three comparison groups with the large significant differential fold change of DEGs were ppm0Vsppm2, ppm2Vsppm5.4, and ppm2Vsppm4. (Fig. 2). The numbers of DEGs in different comparison groups were showed in (Fig. 3). There were 118 DEGs between control group (ppm5.4) and treated group with the lowest level of DO (ppm0). Between group ppm5.4 and ppm2, 56 DEGs were identified. There only 5 DEGs between the group ppm0 and ppm2. But no DEGs were identified between the group ppm5.4 and ppm4.

Transformed count data (Supplementary Information Table S13) was extracted by DESeq2 using the method of variance stabilizing transformation in order to visualization, including clustering, heatmap and principal components analysis (Fig.3, 4, 5). All 20 samples were clustered into two main branches by the 167 DEGs (Fig. 4a, 5). The group ppm0 and ppm2 were clustered into one clade, ppm5.4 and ppm4 were clustered into another. These results indicated that the level of DO might make more serious effects on the brain of *T. rubripes when the concentration of DO was less than* 4 mg O_2/L. In heatmap, 167 DEGs were mainly clustered into 3 clades based on their expression levels (Fig. 4a). About a quarter of the DEGs exhibited high expression levels, suggesting that they could play important roles when *T. rubripes* was under the condition of low DO. Interestingly, range of DEGs fold change was small. There were only 19 DEGs with a fold change of more than 2 (Fig. 4b), and among these 19 DEGs, 16 DEGs were found between the control ppm5.4 and the treatment ppm0 (Fig. 1), which was the largest difference among the comparison groups, followed by when the oxygen concentration was ppm5.4 and ppm2 (Fig. 1). These results indicated that the transcriptomes of brain in *T. rubripes* changed little during acute hypoxia treatment.

Annotation and function analysis of DEGs

The GO classification system grouped the DEGs into three main categories: biological process, cellular component, and molecular function (Fig. 6). The possible roles of DEGs were investigated by GO enrichment analysis. The enrichment analysis showed that most of the DEGs were significantly enriched to the category of biological processes (Fig. 6a). For example, the three terms ("response to steroid hormone", "response to hypoxia", and "response to decreased oxygen levels") were enriched significantly enriched with a high number of DEGs. The next significant enrichment was in the category of molecular function (Fig. 6b), and the top two enriched terms with a high number of DEGs were "dioxygenase activity" and "RNA polymerase II–specific DNA–binding transcription factor binding". However, for the category of cellular components, we found that the number of DEGs enriched was small and insignificant (Fig. 6c). Interestingly, we clustered all these enriched terms and found that they could be well clustered into eight major functional categories (Fig. 7). Among them, most of the significantly enriched terms were clustered into two functional categories, decreased oxygen levels hypoxia and corticosteroid corticosterone death glucocorticoid.

KEGG is a database resource containing many metabolic pathways and their relationships (Kanehisa and Goto 2000). In our study,167 DEGs were grouped into 187 known pathways and the largest group was MAPK signaling pathway, containing 10 DEGs, followed by PI3K-Akt signaling pathway(9), Axon guidance(6), IL-17 signaling pathway (5), HIF-1 signaling pathway(5). Among them, the MAPK signaling pathway enrichment was most significant (Fig. 8). Interestingly, through the network diagram we found that MAPK signaling pathway and PI3K-Akt signaling pathway had the highest degree and connected the most genes（Fig. 9）. For genes, *fos*, *jun*, *rxra*, *vegfa*, and *flt1* had the highest degree and connected the most network pathways. Metabolism-related pathways and genes also clustered well together. In addition, five genes were found to be enriched in HIF-1 signaling pathways related to hypoxia stress: *LOC101071669(egln2), flt1, LOC101079462(hk2), LOC101063282(slc2a1)*, and *vegfa*. Among those HIF-1 signaling pathway-related genes, as the DO concentration decreased, *all five* enriched genes were up-regulated, while *hif1a* did not change significantly.

Validation of DEGs by q RT-PCR

To validate our Illumina sequencing results, 6 genes were selected for q RT-PCR analysis. As shown in （Fig. 10）, although the relative expression levels were not completely consistent, the expression patterns of these genes identified by qRT-PCR were similar to those obtained in RNA-Seq analysis, which indicated the expression data from RNAseq was reliable.

Discussion

Maintaining homeostasis is a key function of the brain, and homeostasis includes blood oxygen levels(van der Velpen et al. 2017). Hypoxia-inducible factor 1α (*hif-1α*) and vascular endothelial growth factor (*vegf*) are activated by hypoxia, which then leads to a disruption of the total blood-brain barrier (BBB), resulting in brain edema (Lafuente et al. 2016; Mohaddes et al. 2017). In mammals, hypoxia is a trigger stimulus for vascular remodeling, altered cell permeability, and angiogenesis (Zimna and Kurpisz 2015). *Vegf* has been proven to be an important determinant of angiogenesis and plays an important role in hypoxic-ischemic brain injury, functioning to promote angiogenesis and neuroprotection (Cao et al. 2018). *Vegf* could stimulate axonal growth and improve neuronal cell survival. Under pathological conditions, *vegf* has a protective effect on the central nervous system (Plaschke et al. 2008). Vascular endothelial growth factor-α (*vegfa*) is a pro-angiogenic member of the vascular endothelial growth factor (*vegf*) family (Ferrara et al. 2003). Here, we showed that *vegfa* was up-regulated with decreasing DO concentration. It participates in the AGE-RAGE signaling pathway. In addition, *egr1*, a gene of the EGR family involved in the AGE-RAGE signaling pathway, showed a decreasing trend. Early growth response 1 (*egr1*) is considered to be a transcription factor sensitive to ischemia and hypoxia. In the brain tissue after ischemic stroke, the mRNA level of *egr1* was significantly increased, while *egr1* was overexpressed induced post-stroke inflammatory response and led to secondary brain damage after cerebral infarction (Tureyen et al. 2008). The main mechanism of the AGE-RAGE signaling pathway is that the interaction between AGE and RAGE causes an oxidative stress response, which in turn promotes the increase in diacylglycerol (DAG) synthesis and activates PKC. Activation of PKC increases the expression of vascular

endothelial growth factor (*vegf*), transforming growth factor-β (*tgf-β*), endothelin-1, and prostaglandin, which proliferates the extracellular matrix, leading to vasomotor dysfunction and capillaries changes in permeability (Ishii et al. 1998; Toth et al. 2008). In our study, under hypoxic stress, *vegfa* expression was up-regulated and *egr1* was down-regulated. It is shown that the brain of *T. rubripes might* create hypoxia tolerance to resist brain damage caused by hypoxia stress.

HIF-1 signaling pathway is a critical pathway during hypoxia. *vegfa* not only mediates the AGE-RAGE signaling pathway but also mediates the HIF-1 signaling pathway. Hypoxia-inducible factor 1 (*hif1*) is a transcription factor expressed in all metazoans and consists of *hif-1*alpha and *hif-1*beta subunits. Under hypoxic conditions, *hif1* regulates the transcription of hundreds of genes in a cell-type-specific manner and was a major regulator in the HIF-1 signaling pathway (Semenza 2007) . In our study, genes enriched for the HIF-1 signaling pathway: *egln2*, *flt1*, *sl2a1*, *vegfa* and hk2 were all up-regulated. However, *hif1* (and *hif1an*) did not show a significant change during hypoxia in our results. In Eurasian perch, *hif1*a mRNA levels were upregulated after acute severe hypoxia exposure in the brain and liver, but not in muscle tissue, whereas significant changes were detected in muscle, but not in the brain and liver after chronic moderate hypoxia exposure (Rimoldi et al. 2012). Ndubuizu et al. demonstrated that despite the lack of *hif1* activation, the relative mRNA levels of *vegf* in the aged cortex significantly increased (Ndubuizu et al. 2010). Fong et al. demonstrated that the knockout of *hif1*α in colon cancer cells had no effect on angiogenesis (Fong 2008). Liu et al. demonstrated that the large yellow croaker (*Larimichthys crocea*) has low hypoxia tolerance compared with other fish species, and the mRNA levels of *hif1α* in its brain did not change markedly under hypoxic conditions (Liu et al. 2018), which was consistent with our results. *Hif1*α is specific for the hypoxia response, and its degradation mediated by three enzymes *egln1*, *egln2*, and *egln3 (Zhang et al. 2019)*. *Tcf7l2* positively regulated aerobic glycolysis by suppressing Egl-9 family hypoxia inducible factor 2 (*egln2*), leading to the upregulation of *hif1*α (Xiang et al. 2018). *Egln2* can hydroxylate *foxo3a* on two specific prolyl residues in vitro and in vivo. Hydroxylation of these sites prevents the binding of USP9x deubiquitinase, thereby promoting the proteasomal degradation of *foxo3a* (Zheng et al. 2014). Flt-1 (*vegfr-1*) and *kdr* (*vegfr-2*) were two highly homologous tyrosine kinase receptors of *vegf*, which can synergize with *vegf* to promote angiogenesis (Gille et al. 2000). Solute Carrier Family 2 Member 1 (*slc2a1*) was the most important energy carrier of the brain: present at the blood-brain barrier and assures the energy-independent, facilitative transport of glucose into the brain(Klepper et al. 1999).The hyperpolarization has been proposed to occur via stimulation of Na^+/K^+ ATPase pumps caused by a glucokinase (*gck*) induced rise of ATP levels within neurons, leading to inhibition of neuronal activity(De Backer et al. 2016). In summary, *hif1*-mediated gene expression may be related to hypoxia-induced tolerance (Jones and Bergeron 2001), or it may be related to the different stresses of different tissues on hypoxia stimulation. *Hif1* was inhibited in the *T. rubripes* brain to prevent brain damage and activate related genes of angiogenesis, promotes blood vessel growth, maintains normal blood vessel density, and was protected from damage caused by ischemia and hypoxia. At the same time, hypoxic stress also promoted the brain to reduce energy consumption.

In our research, we observed that when *T. rubripes* faced with hypoxia, they stopped swimming, laid on the bottom of the tank, and maintained their balance, with only slight swings in the fins. We speculated that the *T. rubripes* had a certain ability to tolerate hypoxia, and it can be made tolerant to hypoxia by changing its activity mode. The central nervous system of vertebrates controls the body's cognitive functions and autonomous motor activities(Paridaen and Huttner 2014). Axon guidance represents a key stage in the formation of neuronal networks (Negishi et al. 2005). Axons were guided by a variety of guidance factors and these guidance cues are read by growth cone receptors, and signal transduction pathways downstream of these receptors converge onto the Rho GTPases to elicit changes in the cytoskeletal organization that determine which way the growth cone will turn (Govek et al. 2005). Recent work in the *D. rerio* has shown that developmental hypoxic injury disrupts pathfinding of forebrain neurons in *D. rerio*, leading to errors in which commissural axons fail to cross the midline. *EphrinB2a* acts as a ligand for one of the receptor tyrosine kinases (RTK) of the *epha3*, *epha4*, or *ephb4* families, which in turn sets off an intracellular signaling cascade in the RTK-expressing cell (Stevenson et al. 2012). Hypoxia stimulated the uptake of 5-bromo-2'-deoxyuridine (BrdU) and reduced cell death Coincident with these proliferative changes, both hif1-α and phospho(p)-AKT were increased while *ephb3* expression was decreased (Baumann et al. 2013). These reports are consistent with our results. Our results showed that the expression of ephb3, ntng1 and rnd1 was down-regulated with decreasing DO concentration, while epha4, sema5b and nck2 appeared to be up-regulated. Among the down-regulated genes, rnd1 was a small signal transduction G protein and a member of the rnd subgroup of the Rho family of GTPases(Ridley 2006). It contributes to the regulation of the actin cytoskeleton in response to extracellular growth factors(Nobes et al. 1998). Ntng1 serves as an axonal guidance cue during vertebrate nervous system development(Nakashiba et al. 2000). Among the up-regulated genes, *sema5b* regulates the development and maintenance of synapse size and number in hippocampal neurons (O'Connor et al. 2009). *Nck2* adaptor proteins were involved in signaling pathways mediating proliferation, cytoskeleton organization, and integrated stress response (Labelle-Cote et al. 2011). From this, we can speculate that the brain of *T. rubripes* may be affected by acute hypoxic stress. However, the brain responded promptly by inhibiting the expression of hif1, reducing the damage caused by hypoxic stress and repairing the damaged nerves in time. This may also be the reason why the brain of *T. rubripes* is able to tolerate hypoxia.

Hypoxia induces *bhlhe40* expression independent of *hif1α* but through a novel p53-dependent signaling pathway, and inhibition of *bhlhe40* or p53 may facilitate muscle regeneration after ischemic injuries (Wang et al. 2015). Studies have shown that prenatal hypoxia in mice can cause continuous changes in circadian rhythms in born mice (Joseph et al. 2002). Hypoxia significantly reduced clock, *cry2*, and *per3* in GF and *cry1*, *cry2*, and *per3* in PDLF (Janjic et al. 2017). Hif-2α increased the expression levels of clock, *bmal1*, *per1*, *cry1*, *cry2*, and *cki*, and decreased the expression levels of *per2* and *per3 (Yu et al. 2015)*. The negative circadian regulator *cry1* was a negative regulator of *hif1a* (Dimova et al. 2019). *Per3* was one of the primary components of circadian clock system. It was found to play a pivotal role in corticogenesis via regulation of excitatory neuron migration and synaptic network formation (Noda et al. 2019). In our study, the expression levels of both genes cry1 and bhlhe40 showed a decreasing

trend due to acute hypoxic stress. Hypoxia has caused brain damage in *T. rubripes* to some extent, thus causing circadian rhythm disturbance in *T. rubripes*. In conclusion, the brain of *T. rubripes* has a certain tolerance to hypoxia, but hypoxia also causes damage to it. Under hypoxic stress, the brain of *T. rubripes* struggles to maintain its central system from damage. Choose to maintain only basic life activities to resist the effects of hypoxic stress, such as stopping swimming to reduce oxygen consumption.

In addition, through the KEGG network interaction map we found that metabolism-related pathways and genes could be well clustered together, including fatty acid metabolism, phosphate metabolism, nitrogen metabolism, bile secretion, and steroid hormone synthesis. *Acl3* encodes a protein that is an isozyme of the long-chain fatty acid coenzyme A ligase family and plays a key role in lipid biosynthesis and fatty acid degradation. And this isozyme is highly expressed in the brain. Furthermore, *acadl*, the gene encoding LCAD (acyl coenzyme A dehydrogenase), has been shown to consume less energy in LCAD-deficient mice and also suffers from hypothermia, which can be explained by the fact that the reduced rate of fatty acid oxidation correlates with a reduced ability to generate heat(Diekman et al. 2014). From this, we can speculate that regulation of energy metabolism may be another effective way for *T. rubripes* to cope with hypoxic stress.

Conclusion

The purpose of this study was to explore the mechanisms of the brain in *T. rubripes* responses to acute hypoxic stress. The transcriptomes of their brain were sequenced and showed small changes under acute hypoxia. We also found that the circadian rhythm, neurodevelopment, and energy metabolism were affected to some extent under acute hypoxic stress. In addition, acute hypoxia also affected the HIF-1 signaling pathway and AGE-RAGE signaling pathway, probably promoting increased cerebral blood flow. Finally, our results indicated that the brain of *T. rubripes* was able to adapt to acute hypoxia and showed high tolerance to acute hypoxia.

Declarations

Funding

This work was supported by the National Key R&D Program of China (2018YFD0900301-10) and the China Agriculture Research System (CARS-47).

Conflicts of interest/Competing interests

The authors declare that they have no competing interests.

Data Availability

All sequencing data were submitted to the Sequence Read Archive (SRA) public database in NCBI (www.ncbi.nlm.nih.gov/), under the accession code PRJNA645780. All other data included in this study

are available upon request by contact with the corresponding author (Yang Liu).

Code availability

Python code for PCA was included in Supplementary Information File S12. Other codes used in this study are available upon request by contact with the corresponding author (Yang Liu).

Authors' contributions.

M. Bao performed the experiments and sampling, initially analyzed the results, and drafted the manuscript. F. Shang further analyzed the experimental results, made graphs and revised the paper. M. Bao and F. Shang contributed equally to this work. F. Liu, Z. Hu, S. Wang, X. Yang, Y. Yu, H. Zhang, C. Jiang, and J. Jiang participated in the experiment and sampling. Y. Liu and X. Wang wrote and reviewed the manuscript. All authors reviewed and approved the final manuscript.

Ethics approval

Animal experiments were approved by the Animal Care and Use committee at Dalian Ocean University.

Consent to participate

All names in the author list have been involved in various stages of experimentation or writing.

Consent for publication

All authors agreed to submit the paper for publication in the Journal of Fish Physiology and Biochemistry.

Acknowledgements

We are very grateful to Dalian Tianzheng Industrial Co. for providing experimental materials and sites.

References

1. Abdel-Tawwab M, Monier MN, Hoseinifar SH, Faggio C (2019) Fish response to hypoxia stress: growth, physiological, and immunological biomarkers Fish. Physiol Biochem 45:997–1013. doi:10.1007/s10695-019-00614-9
2. Anders S, Pyl PT, Huber W (2015) HTSeq–a Python framework to work with high-throughput. sequencing data Bioinformatics 31:166–169. doi:10.1093/bioinformatics/btu638
3. Arend KK et al (2011) Seasonal and interannual effects of hypoxia on fish habitat quality in central Lake. Erie Freshwater Biology 56:366–383
4. Avivi A, Ashur-Fabian O, Amariglio N, Nevo E, Rechavi GJCC (2005) p53–a key player in tumoral and evolutionary adaptation: a lesson from the Israeli. blind subterranean mole rat 4:368–372

5. Avivi A, Resnick MB, Nevo E, Joel A, Levy AP (1999) Adaptive hypoxic tolerance in the subterranean mole rat Spalax ehrenbergi: the role of vascular endothelial growth factor. FEBS Lett 452:133–140. doi:10.1016/s0014-5793(99)00584-0
6. Baumann G, Travieso L, Liebl DJ, Theus MH (2013) Pronounced hypoxia in the subventricular zone following traumatic brain injury and the neural stem/progenitor cell response Experimental biology and medicine 238:830–841 doi:10.1177/1535370213494558
7. Bickler PE, Buck LT (2007) Hypoxia tolerance in reptiles, amphibians, and fishes: life with variable oxygen availability. Annu Rev Physiol 69:145–170. doi:10.1146/annurev.physiol.69.031905.162529
8. Bolger AM, Lohse M, Usadel B (2014) Trimmomatic: a flexible trimmer for Illumina. sequence data Bioinformatics 30:2114–2120. doi:10.1093/bioinformatics/btu170
9. Brenner S, Elgar G, Sandford R, Macrae A, Venkatesh B, Aparicio S (1993) Characterization of the pufferfish (Fugu) genome as a compact model. vertebrate genome Nature 366:265–268. doi:10.1038/366265a0
10. Bruzzi I, Benigni A, Remuzzi G (1997) Role of increased glomerular protein traffic in the progression of renal failure. Kidney international Supplement 62:S29–S31
11. Cao Y et al (2018) Hypoxia-inducible factor-1alpha is involved in isoflurane-induced blood-brain barrier disruption in aged rats model of POCD Behavioural. brain research 339:39–46. doi:10.1016/j.bbr.2017.09.004
12. De Backer I, Hussain SS, Bloom SR, Gardiner JV (2016) Insights into the role of neuronal glucokinase. American journal of physiology Endocrinology metabolism 311:E42–E55. doi:10.1152/ajpendo.00034.2016
13. Diekman EF, van Weeghel M, Wanders RJ, Visser G, Houten SM (2014) Food withdrawal lowers energy expenditure and induces inactivity in long-chain fatty acid oxidation-deficient mouse models. FASEB J 28:2891–2900. doi:10.1096/fj.14-250241
14. Dimova EY et al (2019) The Circadian Clock Protein CRY1 Is a Negative Regulator of HIF-1alpha iScience 13:284–304 doi:10.1016/j.isci.2019.02.027
15. Erkan E, Devarajan P, Schwartz GJ (2007) Mitochondria are the major targets in albumin-induced apoptosis in proximal tubule cells. Journal of the American Society of Nephrology: JASN 18:1199–1208. doi:10.1681/ASN.2006040407
16. Ferrara N, Gerber HP, LeCouter J (2003) The biology of VEGF and its receptors. Nature medicine 9:669–676. doi:10.1038/nm0603-669
17. Fong GH (2008) Mechanisms of adaptive angiogenesis to tissue. hypoxia Angiogenesis 11:121–140. doi:10.1007/s10456-008-9107-3
18. Gille H, Kowalski J, Yu L, Chen H, Pisabarro MT, Davis-Smyth T, Ferrara N (2000) A repressor sequence in the juxtamembrane domain of Flt-1 (VEGFR-1) constitutively inhibits vascular endothelial growth factor-dependent phosphatidylinositol 3'-kinase activation and endothelial cell migration. EMBO J 19:4064–4073. doi:10.1093/emboj/19.15.4064

19. Govek EE, Newey SE, Van Aelst L (2005) The role of the Rho GTPases in neuronal development. Genes Dev 19:1–49. doi:10.1101/gad.1256405
20. Ishii H, Koya D, King GL (1998) Protein kinase C activation and its role in the development of vascular complications in diabetes mellitus. Journal of molecular medicine 76:21–31. doi:10.1007/s001090050187
21. Jackson DC, Ultsch GR (2010) Physiology of hibernation under the ice by turtles and frogs Journal of experimental zoology Part A. Ecological genetics physiology 313:311–327. doi:10.1002/jez.603
22. Janjic K, Kurzmann C, Moritz A, Agis H (2017) Expression of circadian core clock genes in fibroblasts of human gingiva and periodontal ligament is modulated by L-Mimosine and hypoxia in monolayer and spheroid cultures. Archives of oral biology 79:95–99. doi:10.1016/j.archoralbio.2017.03.007
23. Jiang JL, Mao MG, Lu HQ, Wen SH, Sun ML, Liu RT, Jiang ZQ Part D (2017) Digital gene expression analysis of Takifugu rubripes brain after acute hypoxia exposure using next-generation sequencing Comparative biochemistry and physiology. Genomics proteomics 24:12–18. doi:10.1016/j.cbd.2017.05.003
24. Jones NM, Bergeron M (2001) Hypoxic preconditioning induces changes in HIF-1 target genes in neonatal rat brain Journal of cerebral blood flow and metabolism: official. journal of the International Society of Cerebral Blood Flow Metabolism 21:1105–1114. doi:10.1097/00004647-200109000-00008
25. Joseph V, Mamet J, Lee F, Dalmaz Y, Van Reeth O (2002) Prenatal hypoxia impairs circadian synchronisation and response of the biological clock to light in adult rats. J Physiol 543:387–395. doi:10.1113/jphysiol.2002.022236
26. Kai W et al (2011) Integration of the genetic map and genome assembly of fugu facilitates insights into distinct features of genome evolution in teleosts and mammals. Genome Biol Evol 3:424–442. doi:10.1093/gbe/evr041
27. Kanehisa M, Goto S (2000) KEGG: kyoto encyclopedia of genes and genomes. Nucleic acids research 28:27–30. doi:10.1093/nar/28.1.27
28. Kim D, Langmead B, Salzberg SL (2015) HISAT: a fast spliced aligner with low memory requirements. Nat Methods 12:357–360. doi:10.1038/nmeth.3317
29. Klepper J, Wang D, Fischbarg J, Vera JC, Jarjour IT, O'Driscoll KR, De Vivo DC (1999) Defective glucose transport across brain tissue barriers: a newly recognized neurological syndrome. Neurochem Res 24:587–594. doi:10.1023/a:1022544131826
30. Labelle-Cote M, Dusseault J, Ismail S, Picard-Cloutier A, Siegel PM, Larose L (2011) Nck2 promotes human melanoma cell proliferation, migration and invasion in vitro and primary melanoma-derived tumor growth in vivo BMC cancer 11:443 doi:10.1186/1471-2407-11-443
31. Lafuente JV, Bermudez G, Camargo-Arce L, Bulnes S (2016) Blood-Brain Barrier Changes in High Altitude CNS & neurological disorders drug targets 15:1188–1197 doi:10.2174/1871527315666160920123911

32. Liao X, Cheng L, Xu P, Lu G, Wachholtz M, Sun X, Chen S (2013) Transcriptome analysis of crucian carp (Carassius auratus), an important aquaculture and hypoxia-tolerant species. PLoS One 8:e62308. doi:10.1371/journal.pone.0062308
33. Liu W, Liu X, Wu C, Jiang L (2018) Transcriptome analysis demonstrates that long noncoding RNA is involved in the hypoxic response in Larimichthys crocea. Fish Physiol Biochem 44:1333–1347. doi:10.1007/s10695-018-0525-x
34. Liu XZ, Li SL, Jing H, Liang YH, Hua ZQ, Lu GY (2001) Avian haemoglobins and structural basis of high affinity for oxygen: structure of bar-headed goose aquomet haemoglobin Acta crystallographica Section D. Biological crystallography 57:775–783. doi:10.1107/s0907444901004243
35. Livak KJ, Schmittgen TD (2001) Analysis of relative gene expression data using real-time quantitative PCR and the 2 – ΔΔCT. method methods 25:402–408
36. Love MI, Huber W, Anders S (2014) Moderated estimation of fold change and dispersion for RNA-seq data with DESeq. 2 Genome Biol 15:550. doi:10.1186/s13059-014-0550-8
37. Millhorn DE et al (1997) Regulation of gene expression for tyrosine hydroxylase in oxygen sensitive cells by hypoxia. Kidney international 51:527–535. doi:10.1038/ki.1997.73
38. Mohaddes G, Abdolalizadeh J, Babri S, Hossienzadeh F (2017) Ghrelin ameliorates blood-brain barrier disruption during systemic hypoxia. Exp Physiol 102:376–382. doi:10.1113/EP086068
39. Nakashiba T, Ikeda T, Nishimura S, Tashiro K, Honjo T, Culotti JG, Itohara SJJoN (2000) Netrin-G1: a novel glycosyl phosphatidylinositol-linked mammalian netrin that is functionally divergent. from classical netrins 20:6540–6550
40. Ndubuizu OI, Tsipis CP, Li A, LaManna JC (2010) Hypoxia-inducible factor-1 (HIF-1)-independent microvascular angiogenesis in the aged rat brain. Brain research 1366:101–109. doi:10.1016/j.brainres.2010.09.064
41. Negishi M, Oinuma I, Katoh H (2005) Plexins: axon guidance and signal transduction Cellular and molecular life sciences. CMLS 62:1363–1371. doi:10.1007/s00018-005-5018-2
42. Nilsson GE, Renshaw GM (2004) Hypoxic survival strategies in two fishes: extreme anoxia tolerance in the North European crucian carp and natural hypoxic preconditioning in a coral-reef shark. J Exp Biol 207:3131–3139. doi:10.1242/jeb.00979
43. Nobes CD, Lauritzen I, Mattei M-G, Paris S, Hall A, Chardin PJTJocb (1998) A new member of the Rho family, Rnd1, promotes disassembly of actin filament structures and loss of cell adhesion 141:187–197
44. Noda M, Iwamoto I, Tabata H, Yamagata T, Ito H, Nagata KI (2019) Role of Per3, a circadian clock gene. in embryonic development of mouse cerebral cortex Scientific reports 9:5874. doi:10.1038/s41598-019-42390-9
45. O'Connor TP, Cockburn K, Wang W, Tapia L, Currie E, Bamji SX (2009) Semaphorin 5B mediates synapse elimination in hippocampal neurons Neural development 4:18 doi:10.1186/1749-8104-4-18
46. Paridaen JT, Huttner WBJER (2014) Neurogenesis during development of the vertebrate. central nervous system 15:351–364

47. Pelster B, Egg M (2018) Hypoxia-inducible transcription factors in fish: expression, function and interconnection with the circadian clock J Exp Biol 221 doi:10.1242/jeb.163709
48. Plaschke K, Staub J, Ernst E, Marti HH (2008) VEGF overexpression improves mice cognitive abilities after unilateral common carotid artery occlusion. Exp Neurol 214:285–292. doi:10.1016/j.expneurol.2008.08.014
49. Qiu Q et al (2012) The yak genome and adaptation to life at high altitude. Nat Genet 44:946–949. doi:10.1038/ng.2343
50. Rahman MS, Thomas P (2015) Molecular characterization and hypoxia-induced upregulation of neuronal nitric oxide synthase in Atlantic croaker: Reversal by antioxidant and estrogen treatments Comparative biochemistry and physiology Part A. Molecular integrative physiology 185:91–106. doi:10.1016/j.cbpa.2015.03.013
51. Ridley AJ (2006) Rho GTPases and actin dynamics in membrane protrusions and vesicle trafficking. Trends Cell Biol 16:522–529. doi:10.1016/j.tcb.2006.08.006
52. Rimoldi S, Terova G, Ceccuzzi P, Marelli S, Antonini M, Saroglia M (2012) HIF-1alpha mRNA levels in Eurasian perch (Perca fluviatilis) exposed to acute and chronic hypoxia. Molecular biology reports 39:4009–4015. doi:10.1007/s11033-011-1181-8
53. Schmidt R, Weits DA, Feulner CF, Dongen JVJPP (2018) Oxygen sensing and integrative stress signaling in plants:pp.01394.02017
54. Scott GR (2011) Elevated performance: the unique physiology of birds that fly at high altitudes. J Exp Biol 214:2455–2462. doi:10.1242/jeb.052548
55. Semenza GL (2007) Hypoxia-inducible factor 1 (HIF-1) pathway Science's STKE: signal transduction knowledge environment 2007:cm8 doi:10.1126/stke.4072007cm8
56. Shang EH, Wu RS (2004) Aquatic hypoxia is a teratogen and affects fish embryonic development. Environ Sci Technol 38:4763–4767. doi:10.1021/es0496423
57. Shannon P et al (2003) Cytoscape: a software environment for integrated models of. biomolecular interaction networks Genome research 13:2498–2504
58. Simon MC, Keith B (2008) The role of oxygen availability in embryonic development and stem cell function. Nature reviews Molecular cell biology 9:285–296. doi:10.1038/nrm2354
59. Stevenson TJ et al (2012) Hypoxia disruption of vertebrate CNS pathfinding through ephrinB2 Is rescued by magnesium. PLoS Genet 8:e1002638. doi:10.1371/journal.pgen.1002638
60. Ton C, Stamatiou D, Liew CC (2003) Gene expression profile of zebrafish exposed to hypoxia during development. Physiol Genom 13:97–106. doi:10.1152/physiolgenomics.00128.2002
61. Toth C et al (2008) Receptor for advanced glycation end products (RAGEs) and experimental diabetic neuropathy. Diabetes 57:1002–1017. doi:10.2337/db07-0339
62. Tureyen K, Brooks N, Bowen K, Svaren J, Vemuganti R (2008) Transcription factor early growth response-1 induction mediates inflammatory gene expression and brain damage following transient focal ischemia. Journal of neurochemistry 105:1313–1324. doi:10.1111/j.1471-4159.2008.05233.x

63. van der Velpen IF, Feleus S, Bertens AS, Sabayan B (2017) Hemodynamic and serum cardiac markers and risk of cognitive impairment and dementia Alzheimer's & dementia: the. journal of the Alzheimer's Association 13:441–453. doi:10.1016/j.jalz.2016.09.004
64. Vuori KA, Soitamo A, Vuorinen PJ, Nikinmaa M (2004) Baltic salmon (Salmo salar) yolk-sac fry mortality is associated with disturbances in the function of hypoxia-inducible transcription factor (HIF-1alpha) and consecutive gene expression. Aquatic toxicology 68:301–313. doi:10.1016/j.aquatox.2004.03.019
65. Wan QH et al (2013) Genome analysis and signature discovery for diving and sensory properties of the endangered Chinese. alligator Cell research 23:1091–1105. doi:10.1038/cr.2013.104
66. Wang C, Liu W, Liu Z, Chen L, Liu X, Kuang S (2015) Hypoxia Inhibits Myogenic Differentiation through p53 Protein-dependent Induction of Bhlhe40 Protein. J Biol Chem 290:29707–29716. doi:10.1074/jbc.M115.688671
67. Wilhelm BT et al (2008) Dynamic repertoire of a eukaryotic transcriptome surveyed at single-nucleotide. resolution Nature 453:1239–1243. doi:10.1038/nature07002
68. Wu RS, Zhou BS, Randall DJ, Woo NY, Lam PK (2003) Aquatic hypoxia is an disrupter and impairs fish reproduction. Environ Sci Technol 37:1137–1141. doi:10.1021/es0258327
69. Xia JH, Li HL, Li BJ, Gu XH, Lin HR (2018) Acute hypoxia stress induced abundant differential expression genes and alternative splicing events in heart of. tilapia Gene 639:52–61. doi:10.1016/j.gene.2017.10.002
70. Xiang J et al (2018) TCF7L2 positively regulates aerobic glycolysis via the EGLN2/HIF-1alpha axis and indicates prognosis in pancreatic cancer. Cell death disease 9:321. doi:10.1038/s41419-018-0367-6
71. Xie C et al (2011) KOBAS 2.0: a web server for annotation and identification of enriched pathways and diseases. Nucleic Acids Res 39:W316–W322. doi:10.1093/nar/gkr483
72. Yu C, Yang SL, Fang X, Jiang JX, Sun CY, Huang T (2015) Hypoxia disrupts the expression levels of circadian rhythm genes in hepatocellular carcinoma. Mol Med Rep 11:4002–4008. doi:10.3892/mmr.2015.3199
73. Yu G, Wang L-G, Han Y, He Q-Y (2012) clusterProfiler: an R package for comparing biological themes among gene clusters. Omics: a journal of integrative biology 16:284–287
74. Zhang R et al (2019) EGLN2 DNA methylation and expression interact with HIF1A to affect survival of early-stage. NSCLC Epigenetics 14:118–129. doi:10.1080/15592294.2019.1573066
75. Zheng X et al (2014) Prolyl hydroxylation by EglN2 destabilizes FOXO3a by blocking its interaction with the USP9x deubiquitinase. Genes Dev 28:1429–1444. doi:10.1101/gad.242131.114
76. Zimna A, Kurpisz M (2015) Hypoxia-Inducible Factor-1 in Physiological and Pathophysiological Angiogenesis: Applications and Therapies Biomed Res Int 2015:549412 doi:10.1155/2015/549412

Figures

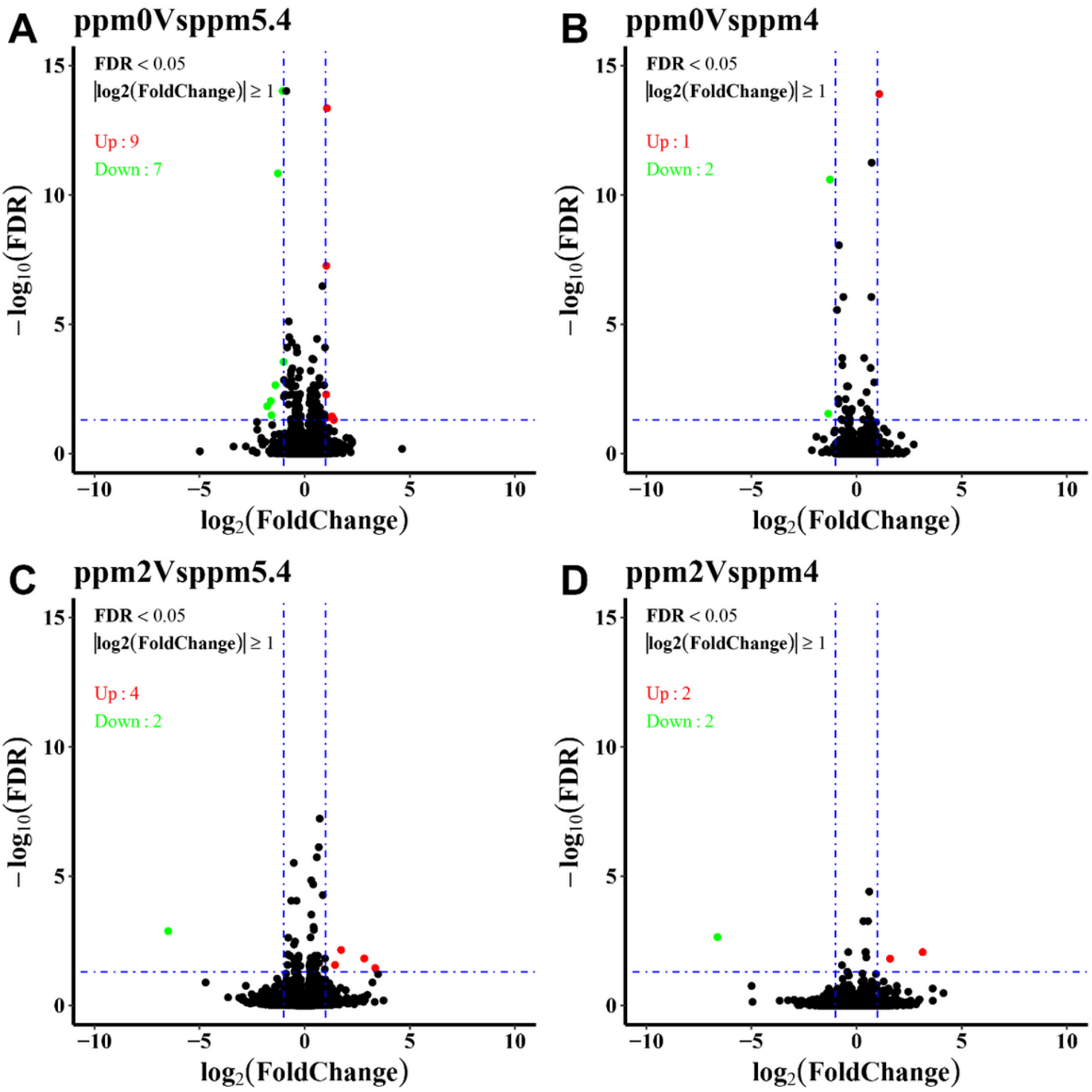

Figure 1

Volcano plot of differentially expressed genes. DEGs with adjusted P value <0.05 and |log2FoldChange|>=1 were chosen for volcano plot in each comparison group. Red points indicated the up-regulated DEGs, and green points indicated down-regulated DEGs.

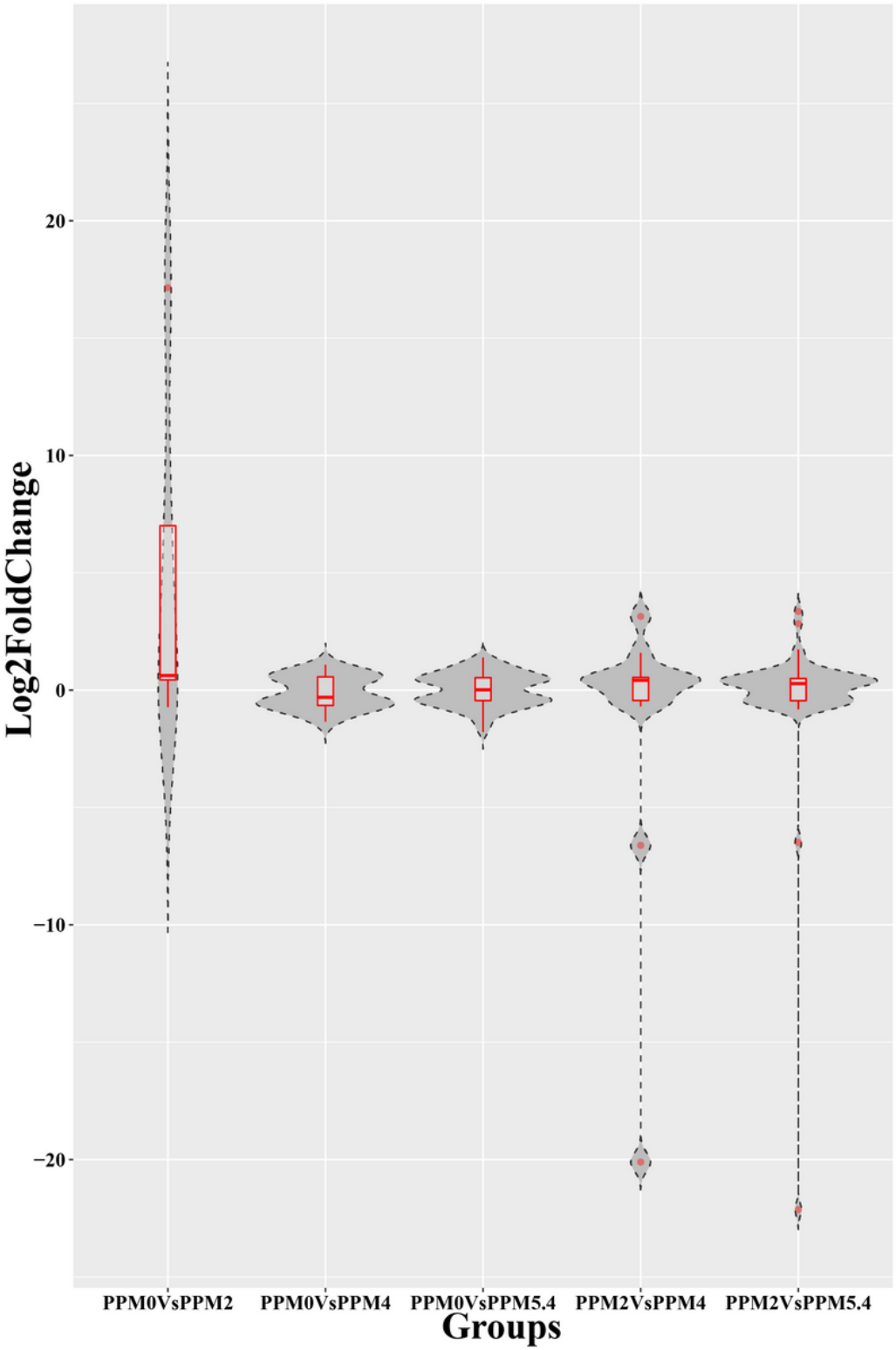

Figure 2

Boxplot and density of the foldchange of differentially expressed genes in each comparison group. The horizontal coordinate indicates the comparison groups between two different oxygen concentrations, and the vertical coordinate indicates the log2(foldchange). log2FoldChange>0 indicates the genes were up-regulated, and log2FoldChange<0 indicates the genes were down-regulated.

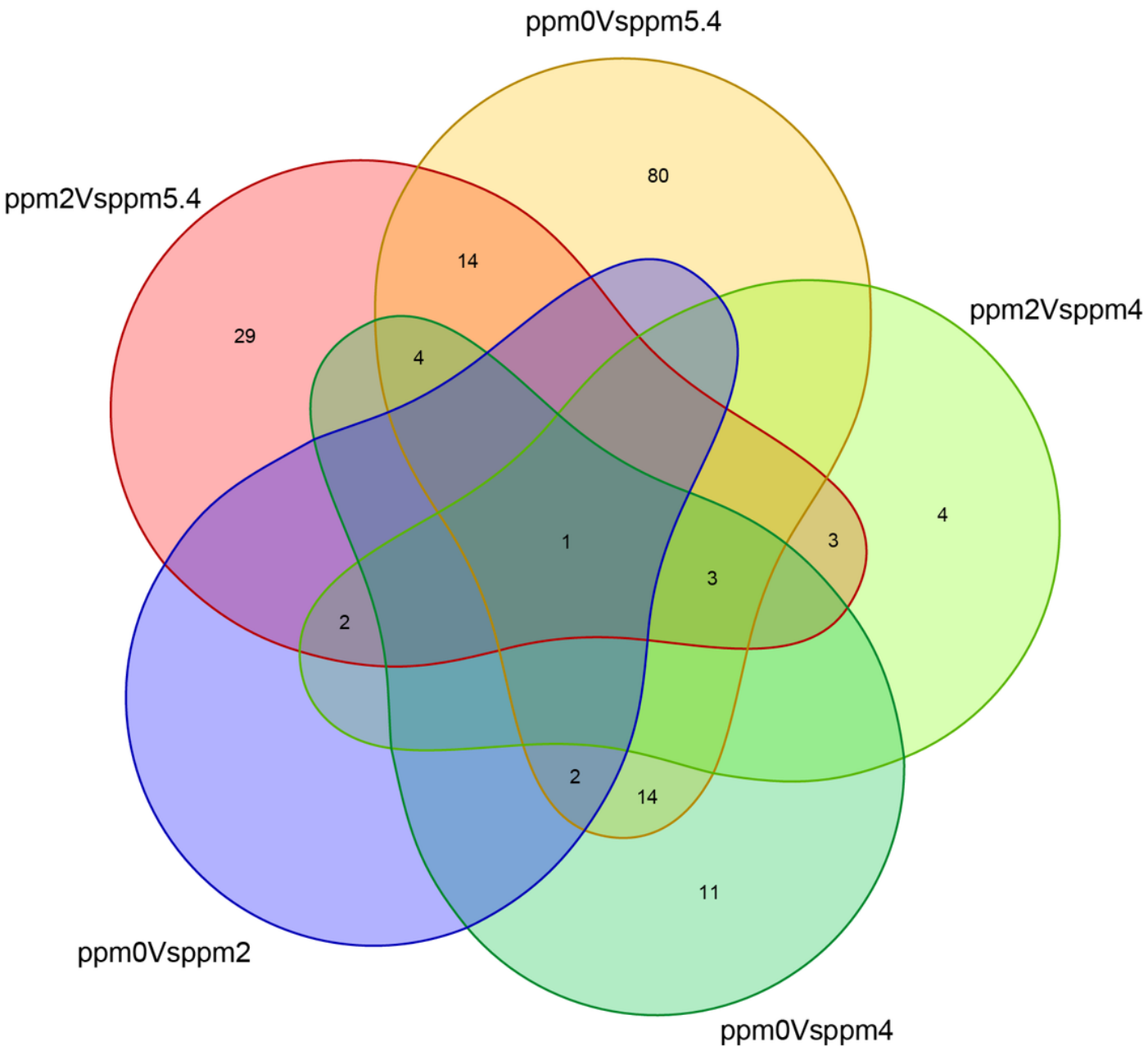

Figure 3

Venn diagram of differentially expressed genes. The comparison groups between two different oxygen concentrations are indicated by different colors. Arabic numbers indicate the number of differentially expressed genes.

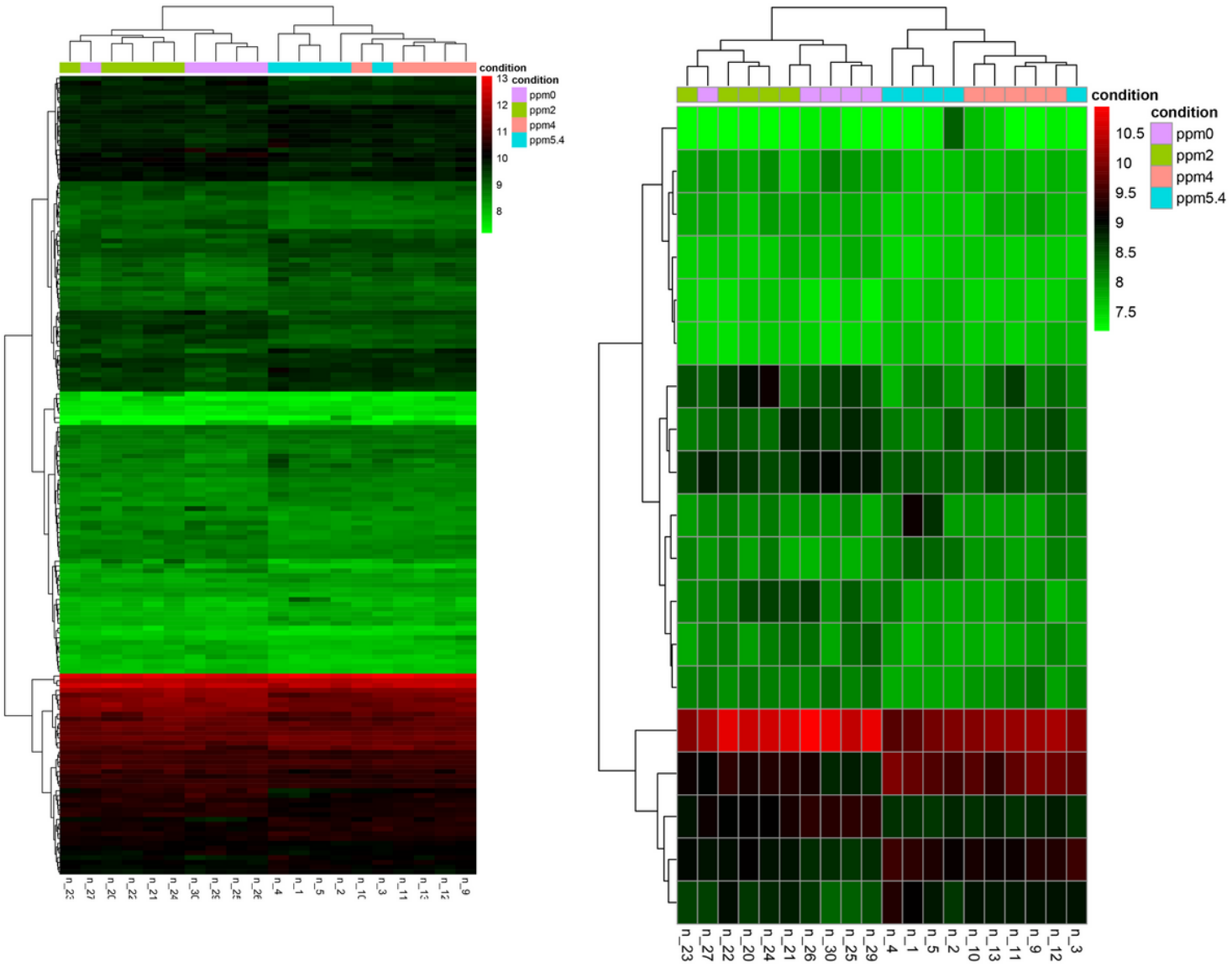

Figure 4

Heatmap of differentially expressed genes. a: DEGs with adjusted P value <0.05 were selected for heatmap. b: DEGs with adjusted P value <0.05 and |log2FoldChange|>=1 were selected for heatmap. Heatmap was drawn based on the normalized expression data (Supplementary Information Table S13). 20 samples were marked under the heatmap.

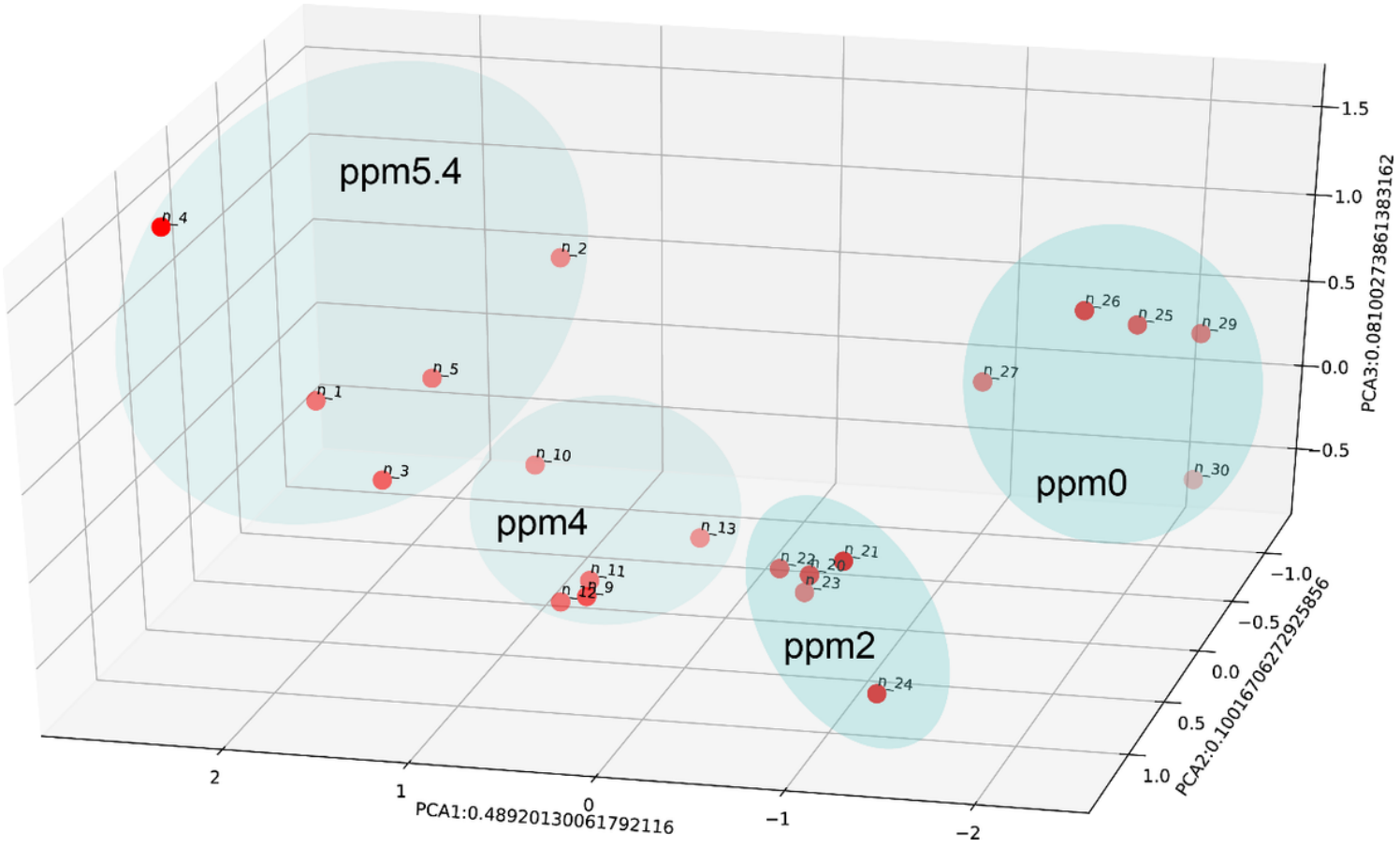

Figure 5

Principal component analysis (PCA) based on the normalized expression data of differentially expressed genes. All 20 samples were shaded by different light blue ellipses indicating the different treatment groups.

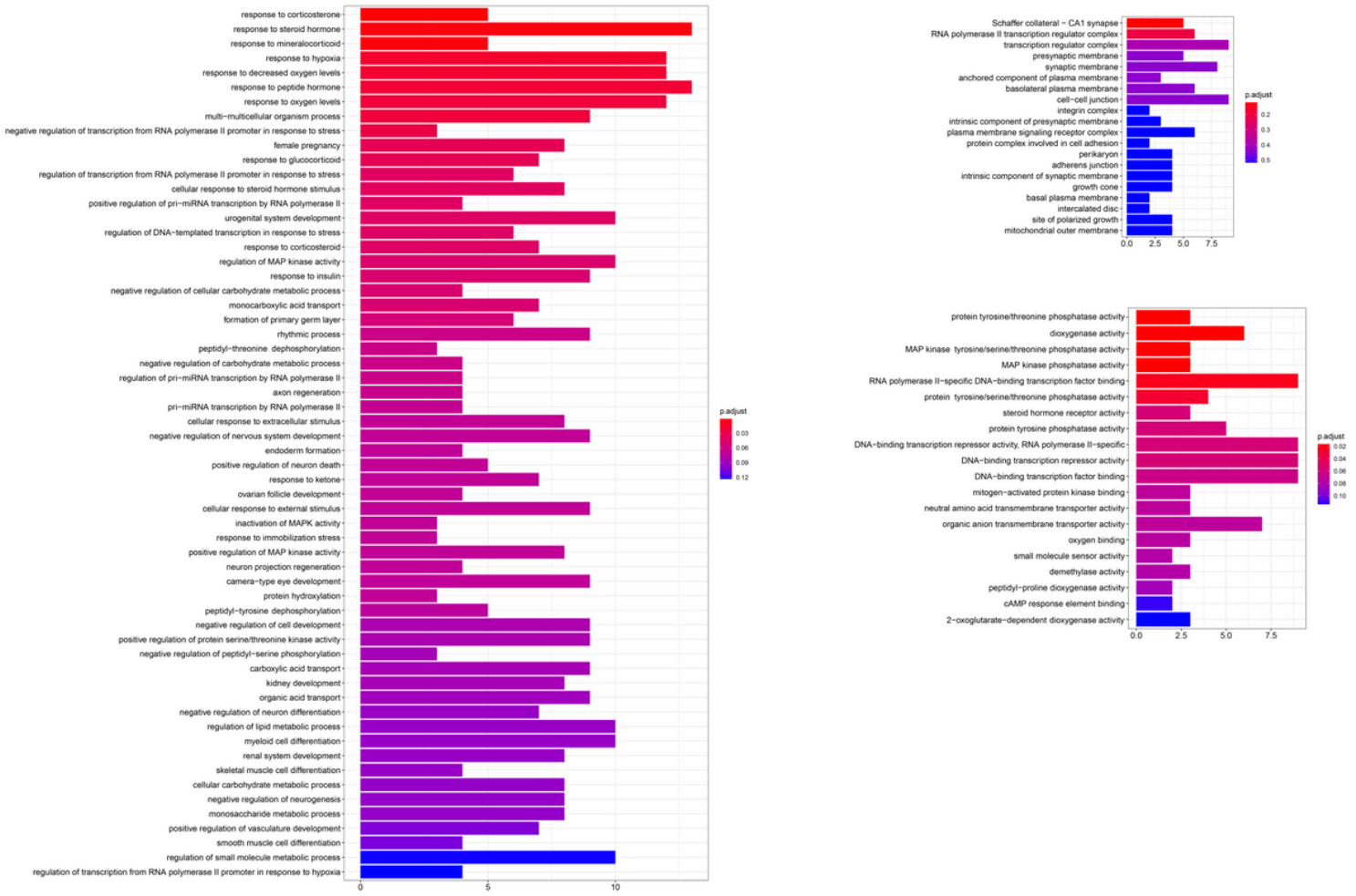

Figure 6

GO enrichment analysis of differentially expressed genes. a: biological processes, b: cellular components, c: molecular functions.

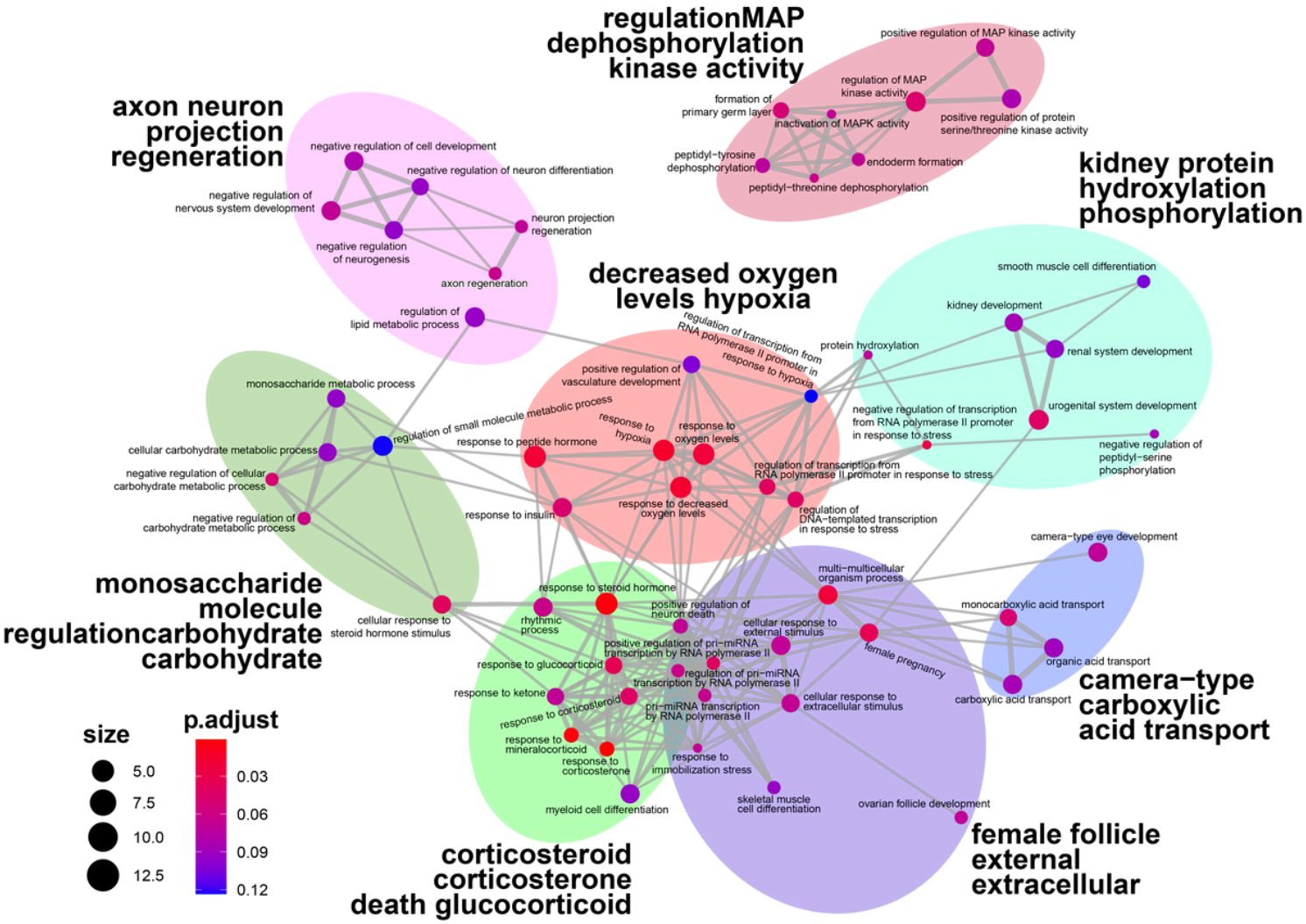

Figure 7

Functional grouping network diagram for GO enrichment analysis. The annotated GO terms were plotted in a network diagram, and the ellipses of different colors in the diagram represented clustered functional groups. Each point represented a GO term.

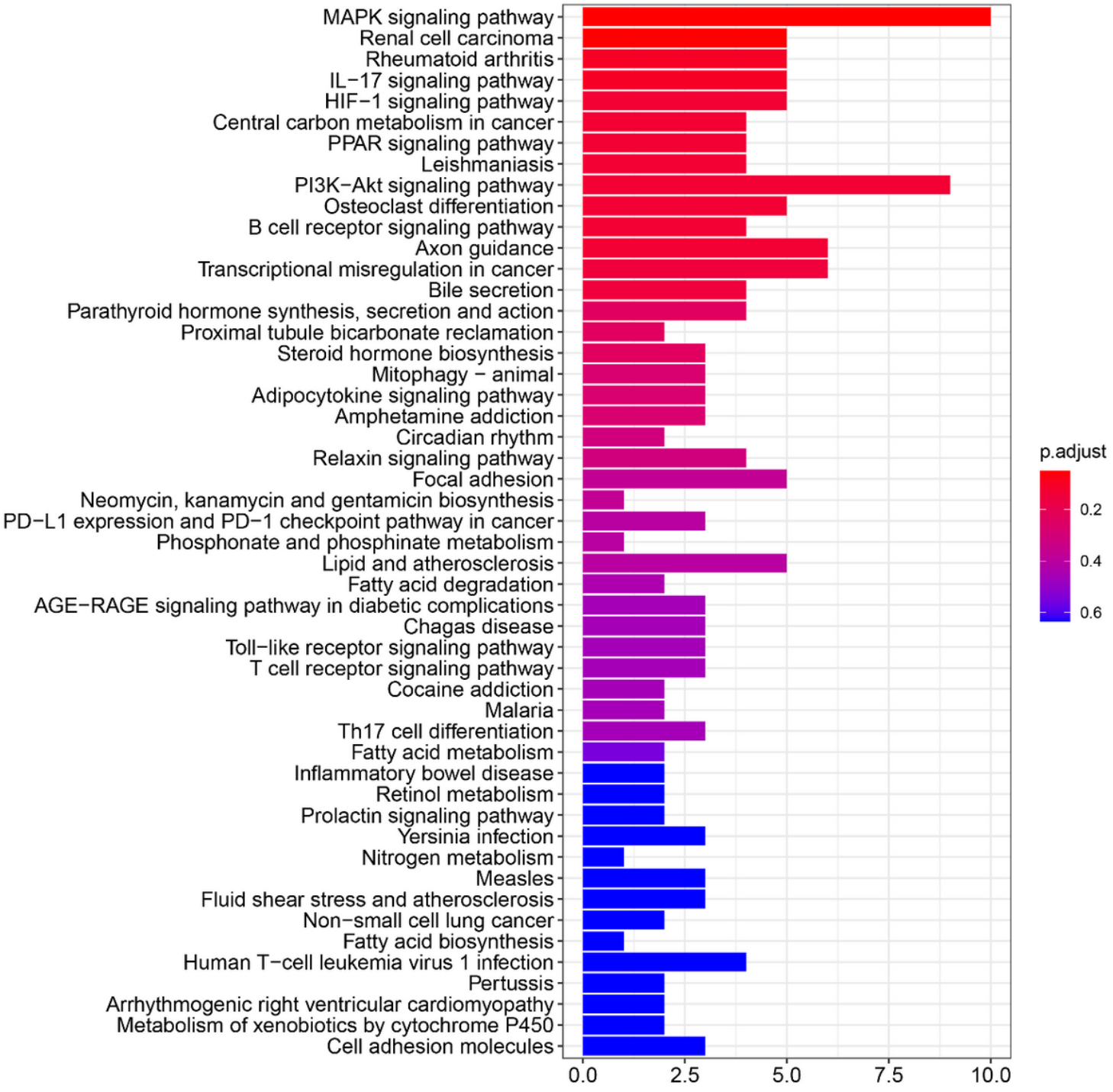

Figure 8

The top 50 enriched KEGG pathways.

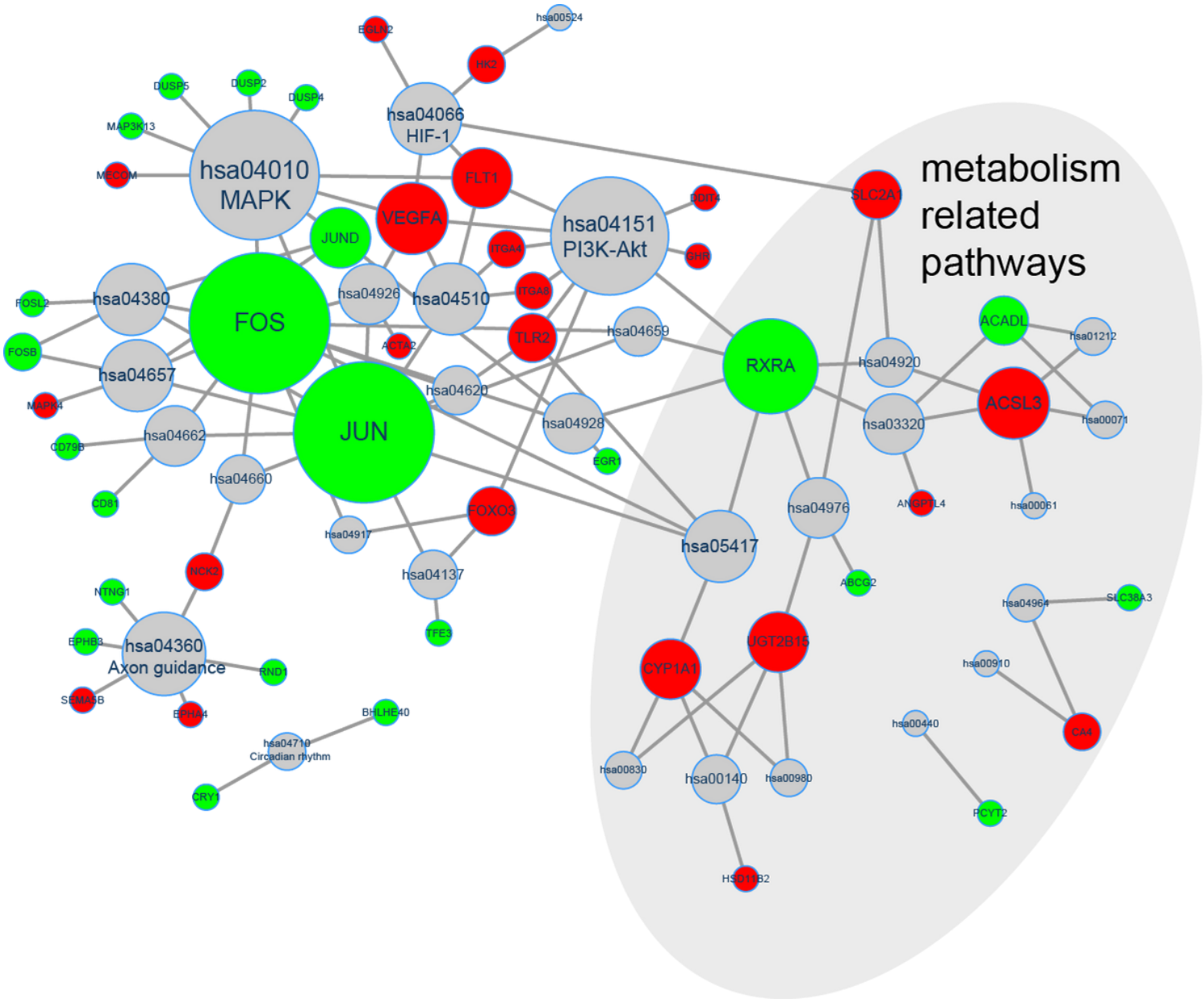

Figure 9

Network of Enriched KEGG pathways and related genes. Red points represented the DEGs with up-regulated trend, green points represented the DEGs with up-regulated trend, and gray points represented enriched KEGG signaling pathway. Enriched metabolism-related pathways were shaded by a gray ellipse. Annotations of KEGG pathway was in Supplementary Information Table S9.

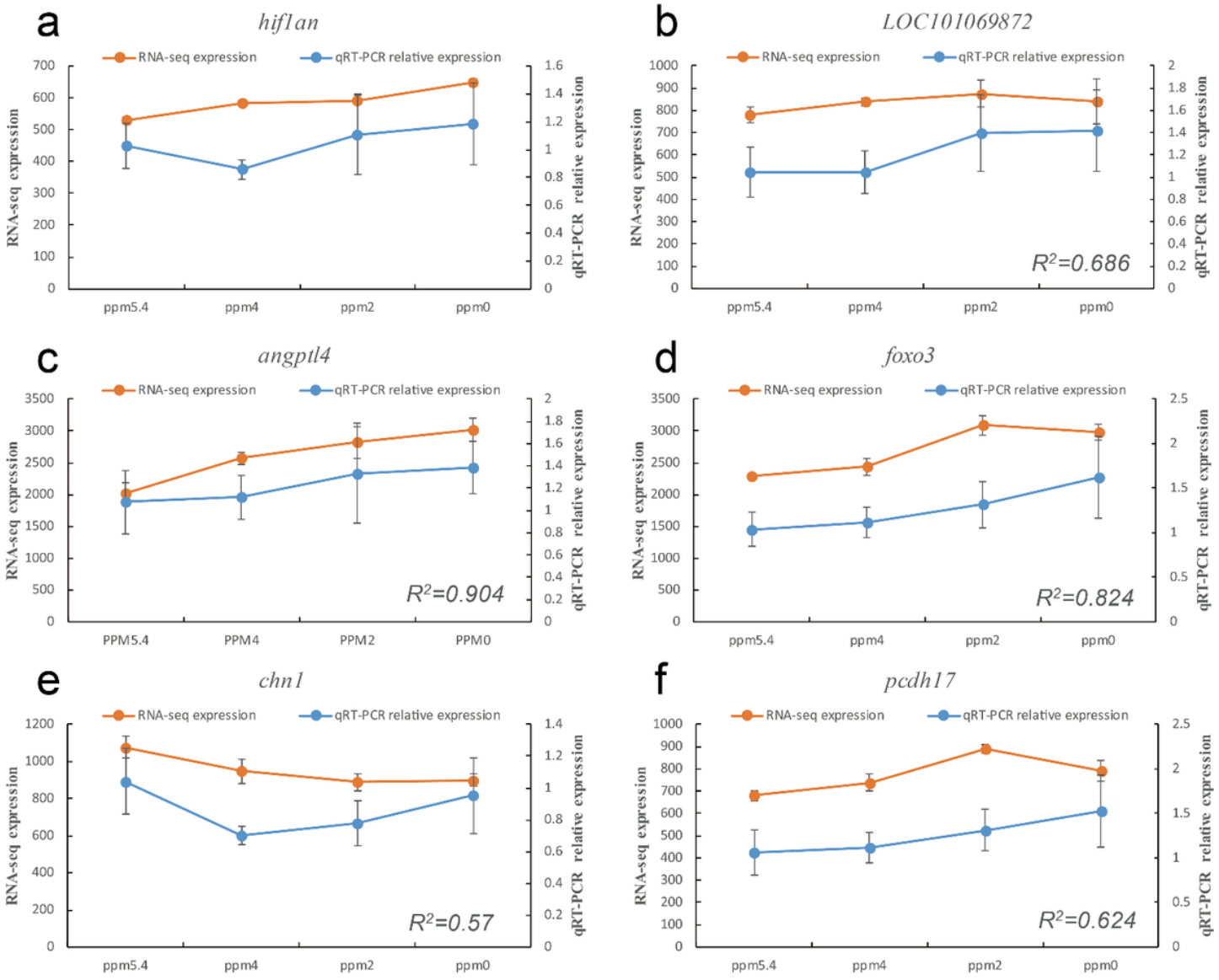

Figure 10

Quantitative real-time PCR verification. The gene expression levels were evaluated relative to the expression level of β-actin using the 2−ΔΔCT method. The correlation between normalized counts from RNAseq and the relative expression from qPCR was calculated.

Supplementary Files

This is a list of supplementary files associated with this preprint. Click to download.

- SupplementaryInformationS1S11S13.xls
- SupplementaryInformationS12pythonPCA3Dplot.py.txt